

EVALUATION OF n + 30Si CROSS SECTIONS FOR THE ENERGY
RANGE 1.0E-11 to 150 MeV

M. B. Chadwick and P. G. Young
1 July 1997

This evaluation provides a complete representation of the nuclear data needed for transport, damage, heating, radioactivity, and shielding applications over the incident neutron energy range from 1.0E-11 to 150 MeV. The discussion here is divided into the region below and above 20 MeV.

INCIDENT NEUTRON ENERGIES < 20 MeV

Below 20 MeV the evaluation is based completely on the ENDF/B-VI.5 (Release 5) evaluation by D. Hetrick, N. Larson, D. Larson, L. Leal, and S. Epperson.

INCIDENT NEUTRON ENERGIES > 20 MeV

The ENDF/B-VI Release 5 evaluation extends to 20 MeV and includes cross sections and energy-angle data for all significant reactions. The present evauation utilizes a more compact composite reaction spectrum representation above 20 MeV in order to reduce the length of the file. No essential data for applications is lost with this representation.

The evaluation above 20 MeV utilizes MF=6, MT=5 to represent all reaction data. Production cross sections and emission spectra are given for neutrons, protons, deuterons, tritons, alpha particles, gamma rays, and all residual nuclides produced ($A>5$) in the reaction chains. To summarize, the ENDF sections with non-zero data above $E_n = 20$ MeV are:

MF=3 MT= 1 Total Cross Section
MT= 2 Elastic Scattering Cross Section
MT= 3 Nonelastic Cross Section
MT= 5 Sum of Binary (n,n') and (n,x) Reactions

MF=4 MT= 2 Elastic Angular Distributions

MF=6 MT= 5 Production Cross Sections and Energy-Angle Distributions for Emission Neutrons, Protons, Deuterons, Tritons, and Alphas; and Angle-Integrated Spectra for Gamma Rays and Residual

Nuclei That Are Stable Against Particle Emission

The evaluation is based on nuclear model calculations that have been benchmarked to experimental data, especially for n + Si28 and p + Si28 reactions (Ch97). We use the GNASH code system (Yo92), which utilizes Hauser-Feshbach statistical, preequilibrium and direct-reaction theories. Spherical optical model calculations are used to obtain particle transmission coefficients for the Hauser-Feshbach calculations, as well as for the elastic neutron angular distributions.

Cross sections and spectra for producing individual residual nuclei are included for reactions. The energy-angle-correlations for all outgoing particles are based on Kalbach systematics (Ka88).

A model was developed to calculate the energy distributions of all recoil nuclei in the GNASH calculations (Ch96). The recoil energy distributions are represented in the laboratory system in MT=5, MF=6, and are given as isotropic in the lab system. All other data in MT=5, MF=6 are given in the center-of-mass system. This method of representation utilizes the LCT=3 option approved at the November, 1996, CSEWG meeting.

Preequilibrium corrections were performed in the course of the GNASH calculations using the exciton model of Kalbach (Ka77, Ka85), validated by comparison with calculations using Feshbach, Kerman, Koonin (FKK) theory [Ch93]. Discrete level data from nuclear data sheets were matched to continuum level densities using the formulation of Ignatyuk (Ig75) and pairing and shell parameters from the Cook (Co67) analysis. Neutron and charged-particle transmission coefficients were obtained from the optical potentials, as discussed below. Gamma-ray transmission coefficients were calculated using the Kopecky-Uhl model (Ko90).

DETAILS OF THE n + SI-30 ANALYSIS

The neutron total cross section above 20 MeV was obtained by evaluating the nat-Si experimental data, with a particular emphasis on the high-accuracy Los Alamos measurements by Finlay (Fi93). The Si-28 total cross section, based on nat-Si data, was scaled by 1.047 (an $A^{2/3}$ factor) for Si-30.

The Madland global medium-energy optical potential (Ma88) was used for neutrons above 46 MeV, and the Wilmore-Hodgson potential was used for lower neutron energies. The Madland global medium-energy optical potential was used for protons above 28 MeV, and the Becchetti-Greenlees potential was used for lower proton energies. In both cases the transition region to the Madland potential was chosen to approximately give continuity in the reaction cross section. For deuterons, the Perey global potential was used; for alpha particles the Moyen potential was used; and for tritons the Becchetti-Greenlees potential was used.

While the above optical potentials did describe the experimental proton nonelastic cross section data fairly well, we modified the theoretical predictions slightly to better agree with the measurements, and renormalized the transmission coefficients accordingly. In addition to using Si nonelastic proton cross section measurements, we also were guided by p+Al nonelastic data, scaled by $A^{2/3}$. The Si-30 nonelastic cross section was taken by scaling the evaluated Si-28 value by 1.047 (an $A^{2/3}$ factor).

Inelastic scattering to the 2+ (2.24 MeV) and 4+ (5.95 MeV) states in 30-Si was determined using a coupled-channel ECIS calculation. To produce continuity in the calculated inelastic cross sections up to 150 MeV, we performed an oblate rotational band (0+, 2+, 4+) coupled channel calculation using the Madland medium energy potential (with its imaginary potential reduced by 20%, to approximately account for the coupling). Deformation parameters were chosen to reproduce the JENDL-3 evaluation at 20 MeV (H.KITAZAWA et al.). The resulting deformation parameters ($\beta_2 = -0.33$, $\beta_4 = 0.20$) were close to those used for Si-28.

The same preequilibrium input parameters were used as for Si-28, which was benchmarked against (n,xz) data from the Louvain group at 63 MeV, and against unpublished (n,xp) data by Haight et al. for neutrons up to 50 MeV. See our ENDF file-1 for n+28Si

for more details.

REFERENCES

- [Be69]. F.D. Becchetti, Jr., and G.W. Greenlees, Phys. Rev. 182, 1190 (1969).
- [Be71]. F.D. Becchetti, Jr., and G.W. Greenlees in "Polarization Phenomena in Nuclear Reactions," (Ed: H.H. Barschall and W. Haeberli, The University of Wisconsin Press, 1971) p.682.
- [Ch93]. M. B. Chadwick and P. G. Young, "Feshbach-Kerman-Koonin Analysis of 93Nb Reactions: P --> Q Transitions and Reduced Importance of Multistep Compound Emission," Phys. Rev. C 47, 2255 (1993).
- [Ch96]. M. B. Chadwick, P. G. Young, R. E. MacFarlane, and A. J. Koning, "High-Energy Nuclear Data Libraries for Accelerator-Driven Technologies: Calculational Method for Heavy Recoils," Proc. of 2nd Int. Conf. on Accelerator Driven Transmutation Technology and Applications, Kalmar, Sweden, 3-7 June 1996.
- [Ch97]. M. B. Chadwick and P. G. Young, "GNASH Calculations of n,p + Si isotopes and Benchmarking of Results" in APT PROGRESS REPORT: 1 June - 1 July 1997, internal Los Alamos National Laboratory memo T-2-97/MS-43, 7 July 1997 from R.E. MacFarlane to L. Waters.
- [Fi93]. R. W. Finlay, W. P. Abfalterer, G. Fink, E. Montei, T. Adami, P. W. Lisowski, G. L. Morgan, and R. C. Haight, Phys. Rev. C 47, 237 (1993).
- [Ma66]. L. MacFadden and G. R. Satchler, Nucl. Phys. 84, 177 (1966).
- [Ma88]. D.G. Madland, "Recent Results in the Development of a Global Medium-Energy Nucleon-Nucleus Optical-Model Potential," Proc. OECD/NEANDC Specialist's Mtg. on Preequilibrium Nuclear Reactions, Semmering, Austria, 10-12 Feb. 1988, NEANDC-245 'U' (1988).
- [Pe63]. C. M. Perey and F. G. Perey, Phys. Rev. 132, 755 (1963).
- [Wi64]. D. Wilmore and P. E. Hodgson, "The Calculation of Neutron Cross Sections from Optical Potentials," Nucl. Phys. 55, 673 (1964).
- [Yo92]. P. G. Young, E. D. Arthur, and M. B. Chadwick, "Comprehensive Nuclear Model Calculations: Introduction to the Theory and Use of the GNASH Code," LA-12343-MS (1992).

14030 = TARGET 1000Z+A (if A=0 then elemental)

1 = PROJECTILE 1000Z+A

Nonelastic, elastic, and Production cross sections for A<5 projectiles in barns:

Energy	nonelas	elastic	neutron	proton	deuteron	triton	helium3	alpha	gamma
2.000E+01	9.712E-01	9.555E-01	1.431E+00	7.360E-02	2.140E-02	1.812E-03	0.000E+00	4.257E-02	1.499E+00
2.200E+01	9.353E-01	1.033E+00	1.392E+00	9.227E-02	2.902E-02	2.762E-03	0.000E+00	5.206E-02	1.496E+00
2.400E+01	9.017E-01	1.094E+00	1.356E+00	1.110E-01	3.213E-01	3.174E-03	0.000E+00	6.293E-02	1.469E+00
2.600E+01	8.695E-01	1.146E+00	1.319E+00	1.264E-01	3.700E-02	3.467E-03	0.000E+00	7.857E-02	1.420E+00
2.800E+01	8.387E-01	1.186E+00	1.295E+00	1.439E-01	4.168E-02	4.155E-03	0.000E+00	7.899E-02	1.353E+00
3.000E+01	8.096E-01	1.219E+00	1.276E+00	1.604E-01	4.596E-02	4.874E-03	0.000E+00	7.960E-02	1.273E+00
3.500E+01	7.448E-01	1.274E+00	1.243E+00	1.986E-01	5.143E-02	6.250E-03	0.000E+00	7.953E-02	1.096E+00
4.000E+01	6.903E-01	1.290E+00	1.209E+00	2.301E-01	5.178E-02	7.270E-03	0.000E+00	8.771E-02	9.926E-01
4.500E+01	6.331E-01	1.286E+00	1.154E+00	2.579E-01	5.241E-02	7.806E-03	0.000E+00	8.364E-02	8.919E-01
5.000E+01	6.007E-01	1.247E+00	1.140E+00	2.880E-01	5.292E-02	8.593E-03	0.000E+00	8.373E-02	8.269E-01
5.500E+01	5.819E-01	1.183E+00	1.148E+00	3.208E-01	5.310E-02	9.612E-03	0.000E+00	8.619E-02	7.991E-01
6.000E+01	5.635E-01	1.112E+00	1.157E+00	3.460E-01	5.424E-02	1.084E-02	0.000E+00	9.301E-02	7.762E-01
6.500E+01	5.467E-01	1.043E+00	1.165E+00	3.680E-01	5.505E-02	1.178E-02	0.000E+00	9.457E-02	7.493E-01
7.000E+01	5.313E-01	9.786E-01	1.170E+00	3.911E-01	5.551E-02	1.285E-02	0.000E+00	9.796E-02	7.124E-01
7.500E+01	5.173E-01	9.088E-01	1.169E+00	4.073E-01	5.659E-02	1.389E-02	0.000E+00	1.010E-01	7.103E-01
8.000E+01	5.044E-01	8.453E-01	1.177E+00	4.234E-01	5.756E-02	1.518E-02	0.000E+00	1.070E-01	6.900E-01
8.500E+01	4.925E-01	7.817E-01	1.182E+00	4.379E-01	5.822E-02	1.615E-02	0.000E+00	1.100E-01	6.735E-01
9.000E+01	4.819E-01	7.295E-01	1.183E+00	4.493E-01	5.944E-02	1.725E-02	0.000E+00	1.129E-01	6.561E-01
9.500E+01	4.723E-01	6.774E-01	1.193E+00	4.628E-01	5.878E-02	1.848E-02	0.000E+00	1.175E-01	6.317E-01
1.000E+02	4.637E-01	6.305E-01	1.195E+00	4.743E-01	6.028E-02	1.961E-02	0.000E+00	1.210E-01	6.129E-01
1.100E+02	4.498E-01	5.512E-01	1.188E+00	4.881E-01	6.218E-02	2.105E-02	0.000E+00	1.231E-01	6.026E-01
1.200E+02	4.402E-01	4.822E-01	1.200E+00	5.077E-01	6.481E-02	2.359E-02	0.000E+00	1.299E-01	5.807E-01
1.300E+02	4.356E-01	4.220E-01	1.231E+00	5.337E-01	6.711E-02	2.648E-02	0.000E+00	1.376E-01	5.567E-01
1.400E+02	4.346E-01	3.696E-01	1.252E+00	5.574E-01	7.094E-02	2.951E-02	0.000E+00	1.437E-01	5.615E-01
1.500E+02	4.374E-01	3.249E-01	1.289E+00	5.850E-01	7.512E-02	3.283E-02	0.000E+00	1.505E-01	5.542E-01

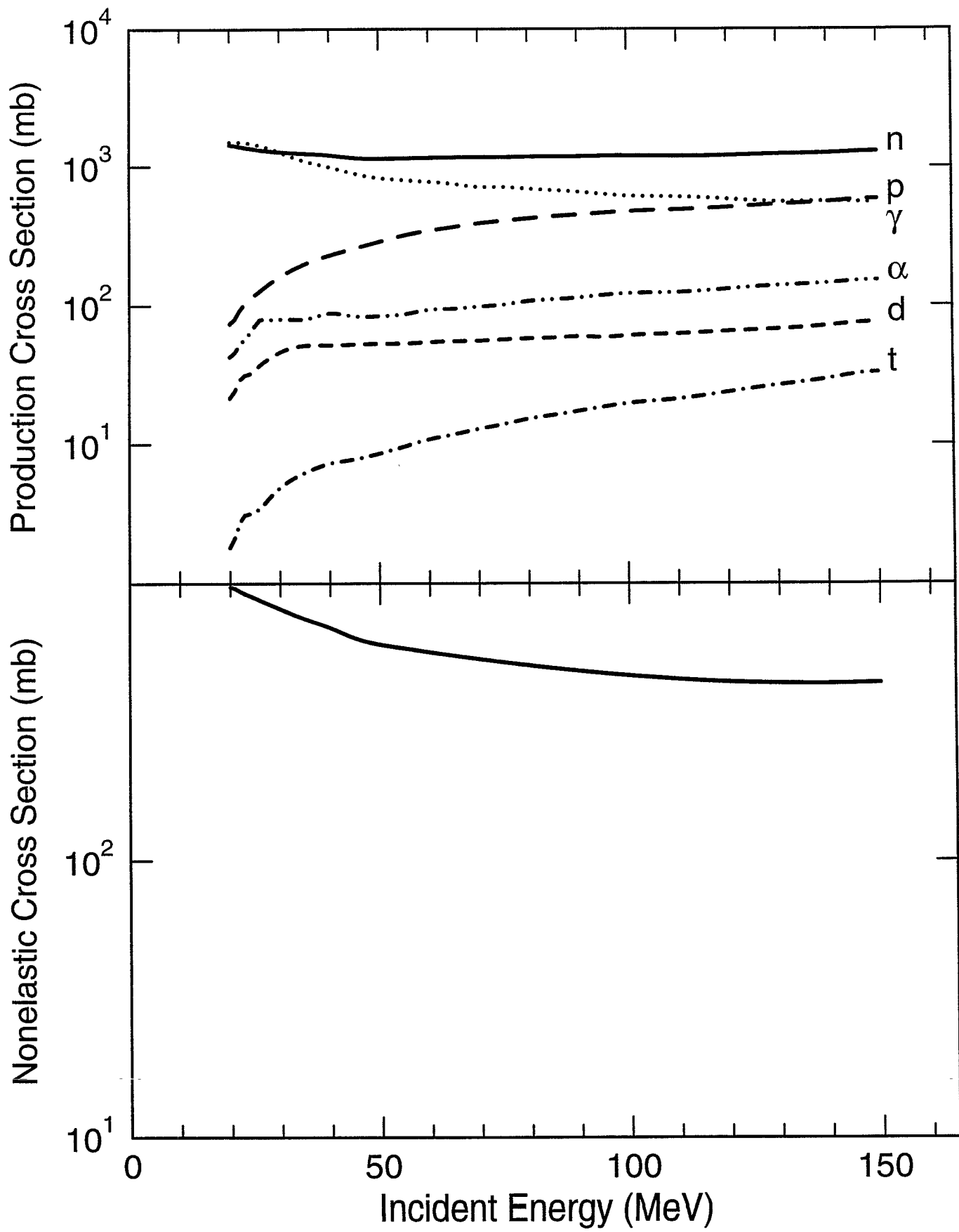
14030 = TARGET 1000Z+A (if A=0 then elemental)

1 = PROJECTILE 1000Z+A

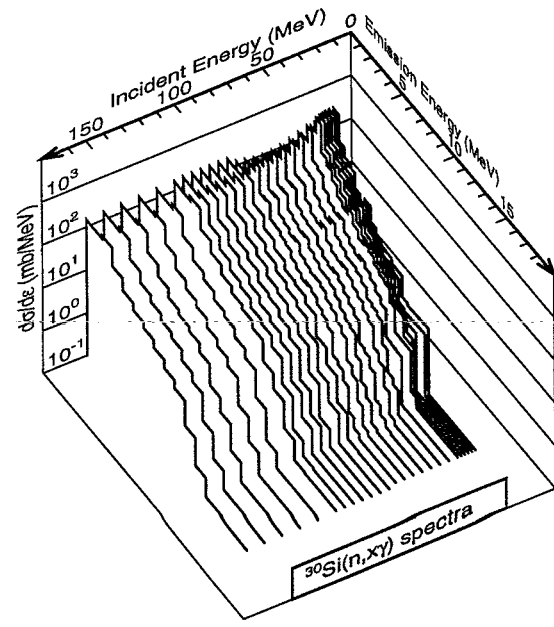
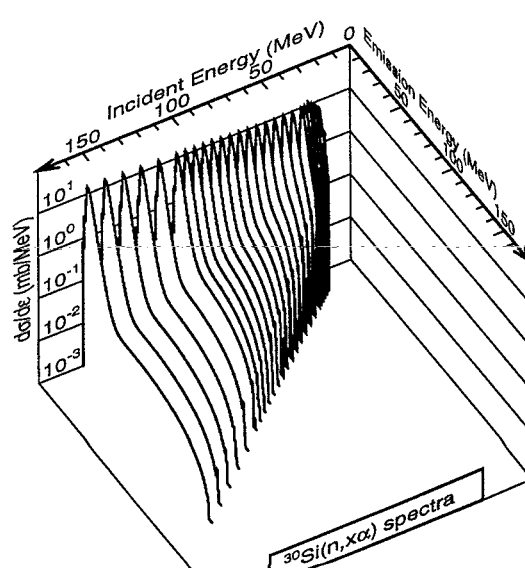
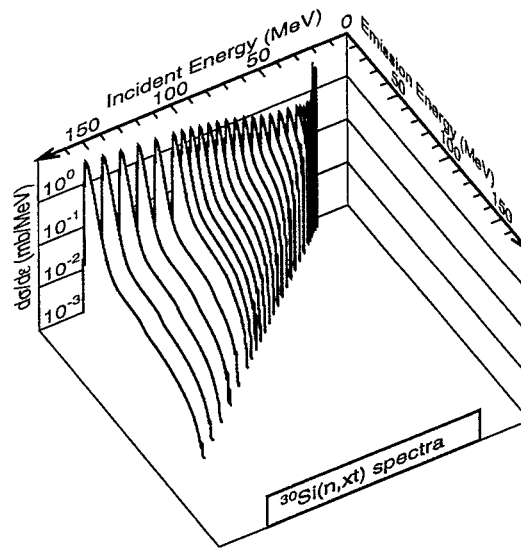
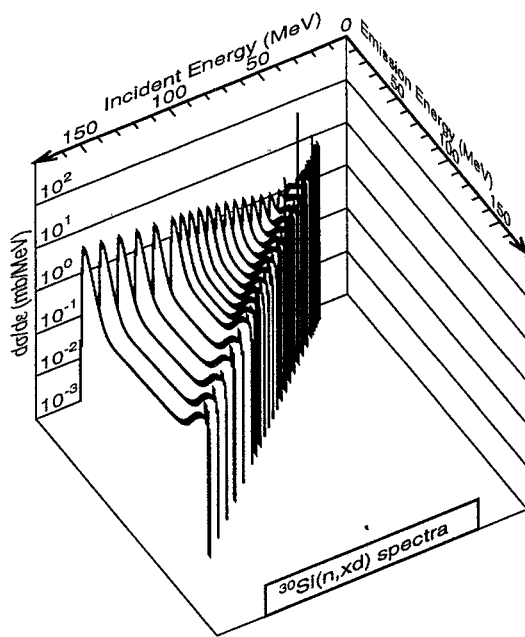
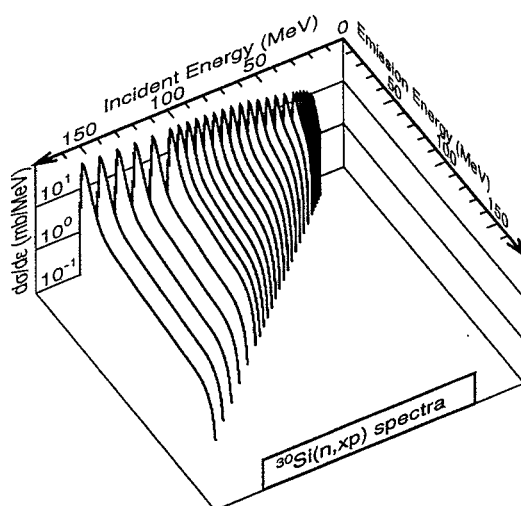
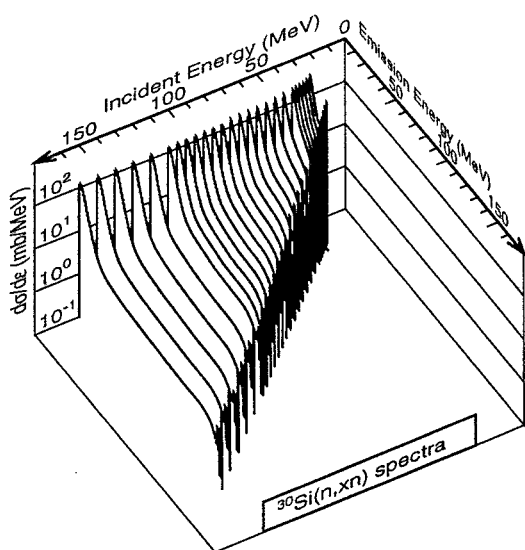
Kerma coefficients in units of f.Gy.m^2:

Energy	proton	deuteron	triton	helium3	alpha	non-rec	elas-rec	TOTAL
2.000E+01	1.341E-01	3.664E-02	1.968E-03	0.000E+00	8.574E-02	2.367E-01	7.215E-02	5.673E-01
2.200E+01	1.814E-01	6.101E-02	3.640E-03	0.000E+00	1.065E-01	2.488E-01	8.611E-02	6.874E-01
2.400E+01	2.325E-01	7.927E-02	4.917E-03	0.000E+00	1.323E-01	2.601E-01	8.571E-02	7.947E-01
2.600E+01	2.857E-01	1.058E-01	6.132E-03	0.000E+00	1.700E-01	2.686E-01	8.442E-02	9.207E-01
2.800E+01	3.496E-01	1.349E-01	8.100E-03	0.000E+00	1.809E-01	2.745E-01	8.237E-02	1.030E+00
3.000E+01	4.165E-01	1.666E-01	1.032E-02	0.000E+00	1.896E-01	2.791E-01	8.000E-02	1.142E+00
3.500E+01	5.951E-01	2.351E-01	1.592E-02	0.000E+00	1.994E-01	2.868E-01	7.372E-02	1.406E+00
4.000E+01	7.657E-01	2.874E-01	2.112E-02	0.000E+00	2.276E-01	2.948E-01	6.712E-02	1.664E+00
4.500E+01	9.280E-01	3.468E-01	2.536E-02	0.000E+00	2.228E-01	2.954E-01	6.134E-02	1.880E+00
5.000E+01	1.111E+00	4.005E-01	2.960E-02	0.000E+00	2.264E-01	3.018E-01	6.988E-02	2.139E+00
5.500E+01	1.320E+00	4.457E-01	3.415E-02	0.000E+00	2.354E-01	3.107E-01	6.277E-02	2.409E+00
6.000E+01	1.506E+00	5.012E-01	3.886E-02	0.000E+00	2.577E-01	3.205E-01	5.652E-02	2.681E+00
6.500E+01	1.701E+00	5.501E-01	4.295E-02	0.000E+00	2.643E-01	3.268E-01	5.128E-02	2.936E+00
7.000E+01	1.890E+00	5.893E-01	4.737E-02	0.000E+00	2.750E-01	3.325E-01	4.689E-02	3.181E+00
7.500E+01	2.070E+00	6.382E-01	5.143E-02	0.000E+00	2.862E-01	3.373E-01	4.266E-02	3.426E+00
8.000E+01	2.241E+00	6.821E-01	5.586E-02	0.000E+00	3.068E-01	3.428E-01	3.903E-02	3.668E+00
8.500E+01	2.423E+00	7.178E-01	5.956E-02	0.000E+00	3.167E-01	3.457E-01	3.563E-02	3.898E+00
9.000E+01	2.599E+00	7.673E-01	6.320E-02	0.000E+00	3.262E-01	3.481E-01	3.290E-02	4.137E+00
9.500E+01	2.792E+00	7.636E-01	6.718E-02	0.000E+00	3.410E-01	3.473E-01	3.029E-02	4.341E+00
1.000E+02	2.966E+00	8.136E-01	7.069E-02	0.000E+00	3.517E-01	3.493E-01	2.799E-02	4.579E+00
1.100E+02	3.341E+00	9.093E-01	7.533E-02	0.000E+00	3.598E-01	3.498E-01	2.421E-02	5.060E+00
1.200E+02	3.724E+00	9.936E-01	8.292E-02	0.000E+00	3.833E-01	3.551E-01	2.101E-02	5.559E+00
1.300E+02	4.158E+00	1.043E+00	9.155E-02	0.000E+00	4.118E-01	3.671E-01	1.826E-02	6.089E+00
1.400E+02	4.599E+00	1.142E+00	1.005E-01	0.000E+00	4.366E-01	3.924E-01	1.589E-02	6.687E+00
1.500E+02	5.095E+00	1.240E+00	1.107E-01	0.000E+00	4.625E-01	4.195E-01	1.386E-02	7.342E+00

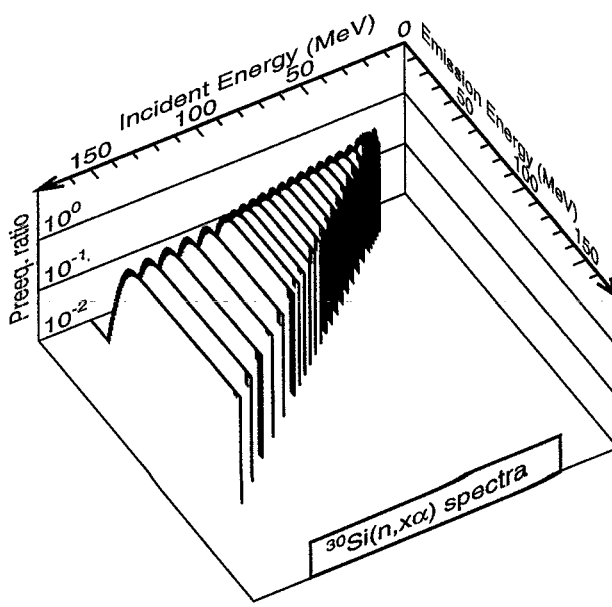
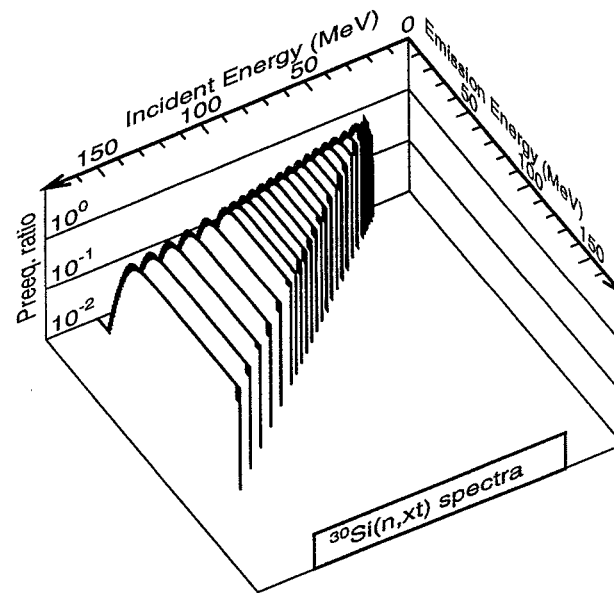
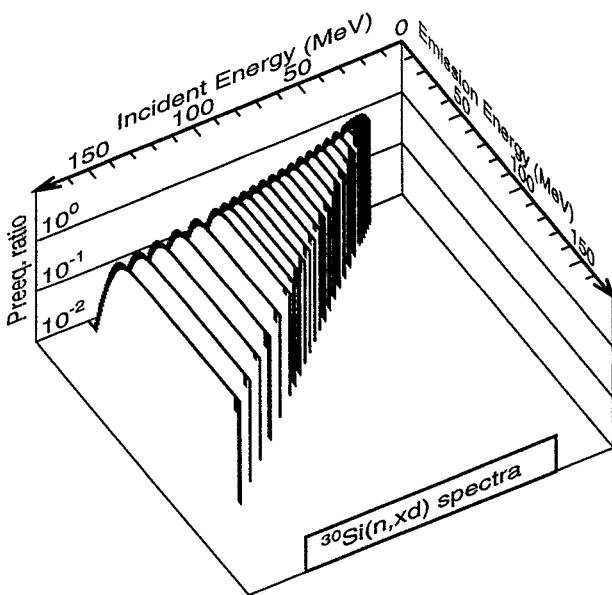
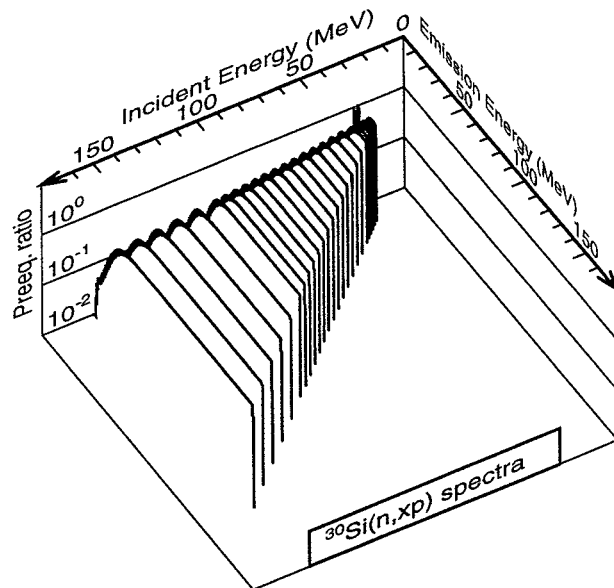
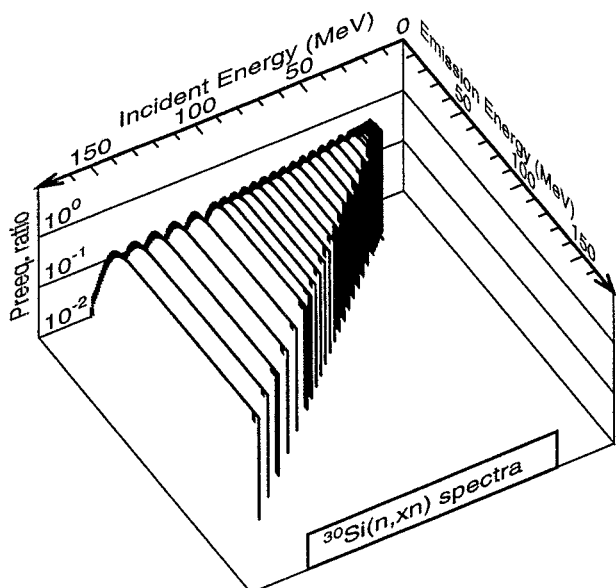
$n + {}^{30}\text{Si}$ nonelastic and production cross sections



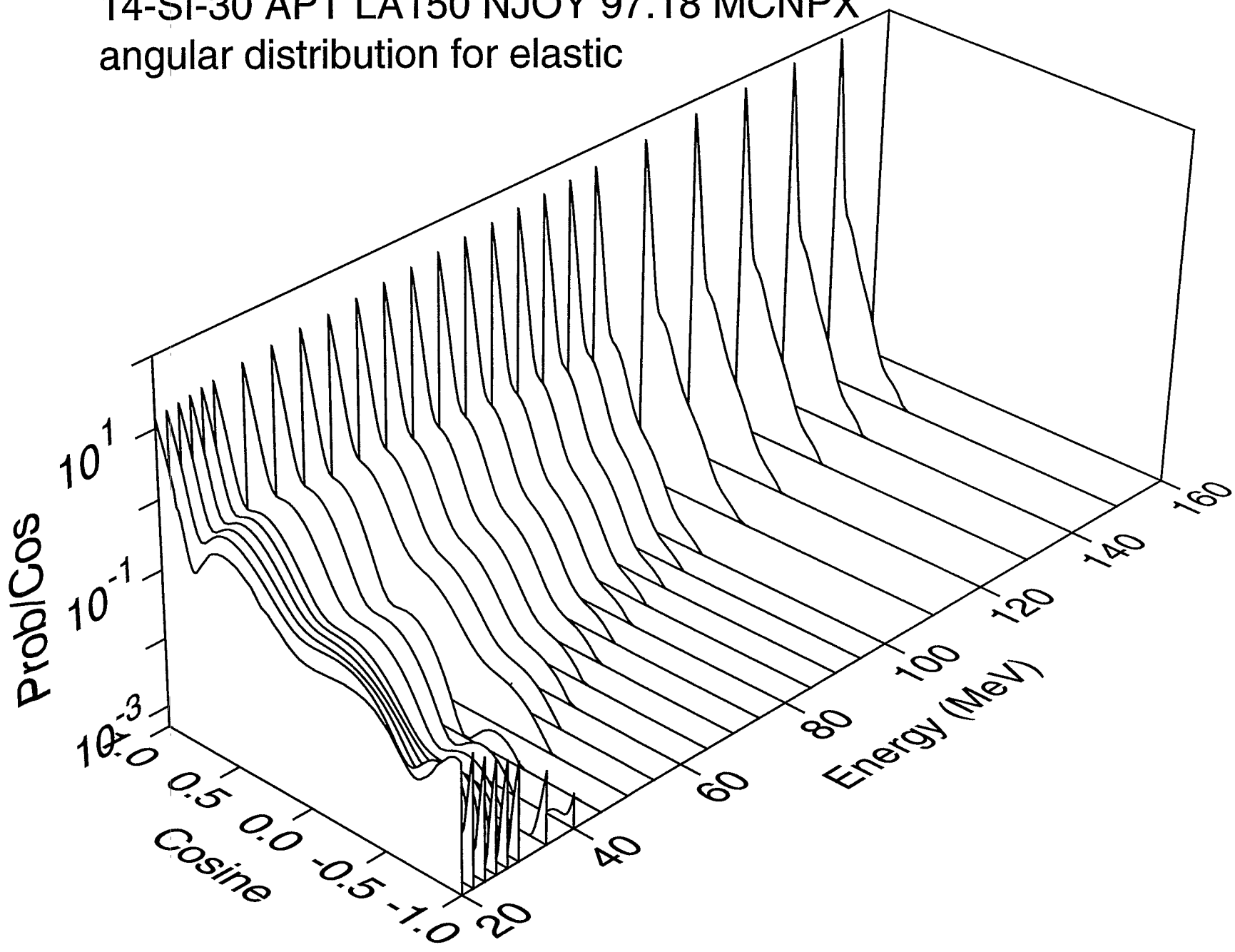
$n + {}^{30}\text{Si}$ angle-integrated emission spectra



$n + {}^{30}\text{Si}$ Kalbach preequilibrium ratios

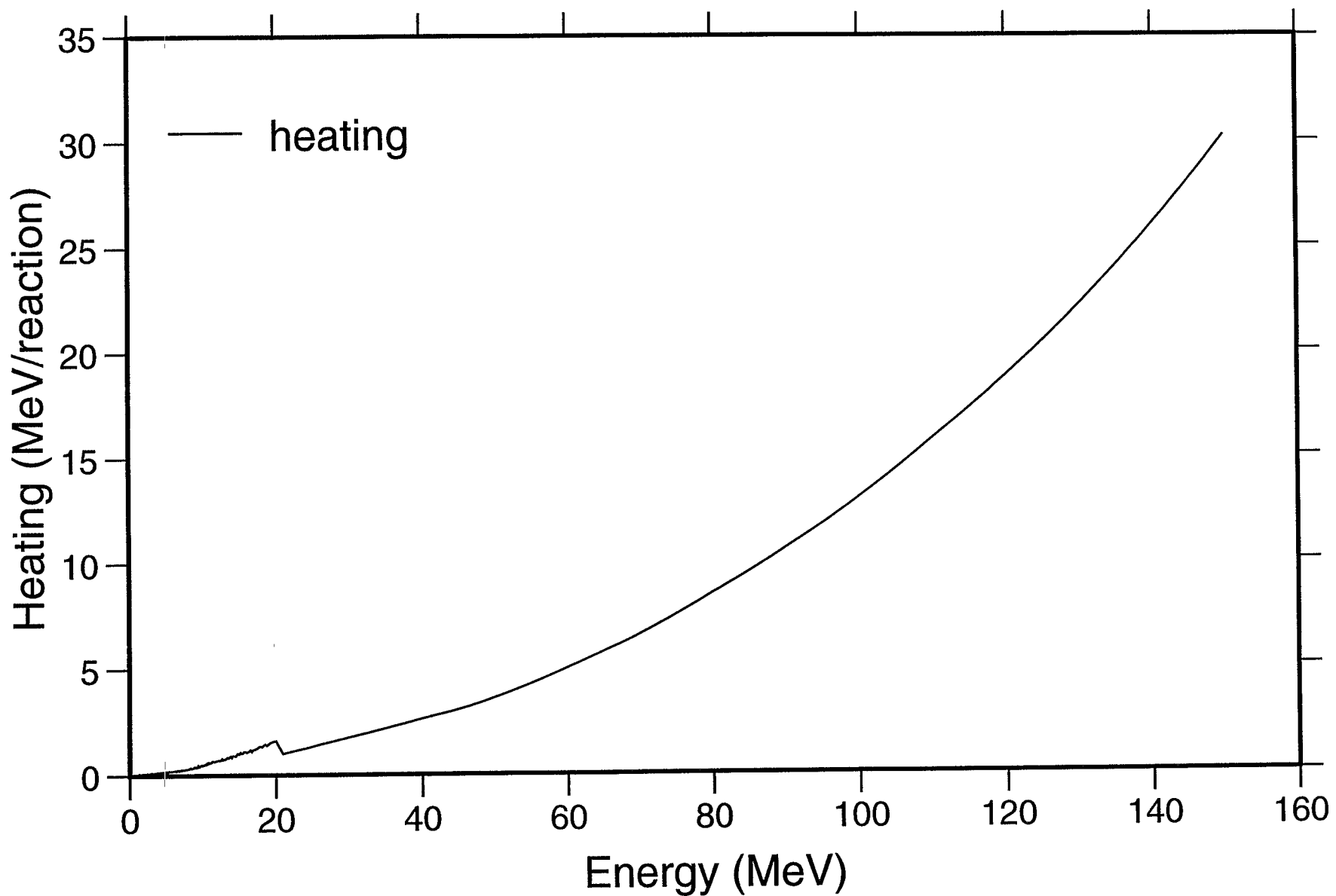


14-SI-30 APT LA150 NJOY 97.18 MCNPX
angular distribution for elastic



14-SI-30 APT LA150 NJOY 97.18 MCNPX

Heating



14-SI-30 APT LA150 NJOY 97.18 MCNPX

Damage

